Available online at www.sciencedirect.com
SCIENCE DIRECT®
Chemical Physics Letters 366 (2002) 205–210
CHEMICAL PHYSICS LETTERS
www.elsevier.com/locate/cplett

Near-infrared-to-visible photon upconversion in Mo-doped rutile titania

Changfeng Wu, Weiping Qin *, Guanshi Qin, Shihua Huang, Jisen Zhang, Dan Zhao, Shaozhe Lü, Huangqing Liu

Key Laboratory of Excited State Processes, Changchun Institute of Optics, Fine Mechanics and Physics, Chinese Academy of Sciences, Changchun 130021, PR China

Received 17 July 2002; in final form 6 September 2002

Abstract

A broadband upconversion luminescence was observed from Mo-doped titania under a 978 nm diode laser excitation. The luminescence has been assigned to the transitions from the excited states $^3T_1$, $^3T_2$ to the ground state $^1A_1$ of the $[MoO_4]^{2-}$ radicle. The intermediate states available for upconversion are supposed to be related with Mo^{4+} and/or Mo^{5+} species. The temporal evolution of the upconversion luminescence and the excitation-power dependence of the steady-state emission intensity exhibit the typical fingerprint of a photon avalanche. The dynamical process is well described using the fluorescence 'transfer function' model.

1. Introduction

For many years, much attention has been given to the study of photon upconversion which are of great fundamental research interest and lead to many applications, for example, in coherent laser light sources [1], 3-D imaging materials [2], or enhanced IR quantum counters [3]. So far most of the investigations have concentrated on some rare earth (RE) ions. Güdel and co-workers [4] initiated a systematic study on transition-metal (TM) ions including Mn^{2+}, Ni^{2+} [5], Mo^{3+} [6], Re^{4+} [7], and Os^{4+} [8], thus expanded the family of upconversion systems. In contrast to the RE ions, the spectroscopically active d orbitals of TM ions are involved in metal–ligand bonding, and so are subject to significant electron–phonon interactions. As a result, the luminescence from most of TM ions is relatively weak. However, the environmental sensitivity of these ions suggests that their photophysical properties may be modified or even controlled using external chemical redox, or magnetic perturbations [9].

Titania is a good candidate to be used as a doping host because of its good mechanical, thermal, and anticorrosive properties [10,11]. In this Letter, we report the upconversion luminescence from Mo-doped titania. The upconversion shows a characteristic of photon avalanche. The avalanche dynamics was analyzed by using the fluorescence 'transfer function' theory.

* Corresponding author. Fax: +86-431-593-7614.
E-mail address: wpqin@public.cc.jl.cn (W. Qin).

0009-2614/02/$ - see front matter
PII: S0009-2614(02)01559-2

2. Experimental

The samples were prepared by high-temperature solid-state reaction. The starting materials were powdered TiO_2 (A.R.) and molybdenum (99.5% purity) at the molar ratio of 97:3. The batch was mixed, placed in an alumina crucible, and calcined in oxidizing atmosphere at 1200 °C for 3 h. Then the sample was annealed at 700 °C for 1 h under reducing atmosphere produced by active carbon. The annealing treatment is indispensable for the material to show upconversion.

X-ray powder diffraction (XRD) analysis, presented in the inset of Fig. 1, proved the as annealed sample was single rutile phase. Infrared absorption spectrum in KBr suspensions was measured by a Bio-Rad Fourier transform infrared (FTIR) spectrometer. The Mo ($3d_{5/2}$) electron binding energies were obtained from X-ray photoelectron spectroscopy (XPS) using a VG Escalab MK Π photoelectron spectrometer. According to the XPS measurements, the element ratio of Mo:Ti was calculated to be 3.29:96.71, close to the stoichiometry of the starting materials. Upconversion spectrum was measured with a Hitachi F-4500 fluorescence spectrophotometer under a 978 nm diode laser (LD, 2W) excitation. By chopping the laser beam at an appropriate speed, time evolution of the upconversion luminescence was recorded by monitoring the output of a R456 photomutliplier tube with a Tektronix TDS 3052 digital oscilloscope. All the measurements were performed at room temperature.

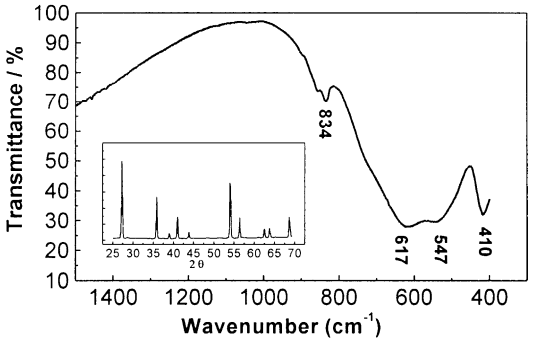

Fig. 1. FTIR spectrum of Mo-doped titania. The inset shows the X-ray diffraction pattern.

3. Results and discussions

3.1. Valence states of Mo ions in the sample

To explain the origin of the luminescence, it is necessary to discern the configuration and valence states of the Mo ions in TiO_2 host. Fig. 1 presents the FTIR spectrum of the TiO_2:Mo material, which confirms the existence of the $[MoO_4]^{2-}$ complexes. Studies of the $[MoO_4]^{2-}$ anion in aqueous solutions have located its fundamental frequencies at 894 ($v_1(A_1)$), 318 ($v_2(E)$), 833 ($v_3(F_2)$), and 407 cm^{-1} ($v_4(F_2)$) [12]. Studies of the solid compounds have shown that the stretching multiplets (v_1 and v_3) occur in the 750–1000 cm^{-1} range and the bending modes in the 250–430 cm^{-1} range for molybdates where anions form isolated tetrahedra. The hexa-coordinated compounds is featured by the new bands in the region 500–750 cm^{-1}, originated from the oxygen bridge bond vibrations [13]. Two sharp peaks at 834 and 410 cm^{-1} were observed in Fig. 1. Obviously, they should be, respectively, assigned to the fundamental frequencies v_3 and v_4 of the $[MoO_4]^{2-}$ anion. The absorption band in the 500–700 cm^{-1} range is attributed to the hexa-coordinated Mo–O complexes or other Mo–O species.

An annealing under reducing conditions is essential for upconversion. Undoubtedly, the $[MoO_4]^{2-}$ complexes had formed before the annealing. The FTIR spectrum proves that they still exist in the as annealed samples. However, the XPS measurements indicate that the annealing transforms part of the Mo ions from hexavalence state into lower valence states. The Mo ($3d_{5/2}$) binding energies of 232.5 and 230.9 eV were reported, respectively, for the hexavalence in MoO_3 and tetravalence in MoO_2. Furthermore, the binding energies increase as the oxidation state of molybdenum becomes more positive, which presents a linear relationship [14]. Fig. 2a gives the Mo ($3d_{5/2}$) electron spectra for TiO_2:Mo sample before annealing. The Mo ($3d_{5/2}$) binding energy was determined to be 232.4 eV, very close to that for hexavalence in MoO_3. For the sample after annealing, the peak position locates at 231.9 eV, as

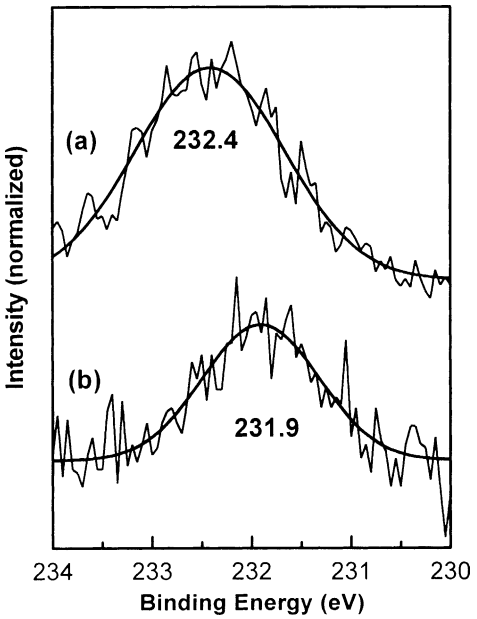

Fig. 2. Molybdenum ($3d_{5/2}$) electron spectra for TiO_2:Mo sample (a) before annealing and (b) after annealing. The smooth lines were reproduced by Gaussian fitting.

shown in Fig. 2b. Compared with the 1.6 eV shift in $3d_{5/2}$ electron binding energy between MoO_3 and MoO_2, the annealing causes a 0.5 eV shift. The value for the annealed sample cannot agree with any single oxidation state, which indicates that the states of the Mo species and their contents are complicated, and may not be definitely determined from our experiments. However, the XPS measurements do suggest that some lower valence states, mainly tetravalence and/or pentavalence, co-exist in the as annealed sample besides the hexavalence within $[MoO_4]^{2-}$ type.

3.2. Upconversion luminescence of TiO_2:Mo

Fig. 3 presents the upconversion luminescence spectrum of TiO_2:Mo under a 978 nm LD excitation. The peak position and lineshape closely resemble those of the luminescent $[MoO_4]^{2-}$ complexes. The molecular orbital energy scheme for free tetrahedral $[MoO_4]^{2-}$ complex was described by means of an extended Hückel method [16]. It is a closed shell configuration with an $^1A_1$ ground state. For the lowest energy electron transition

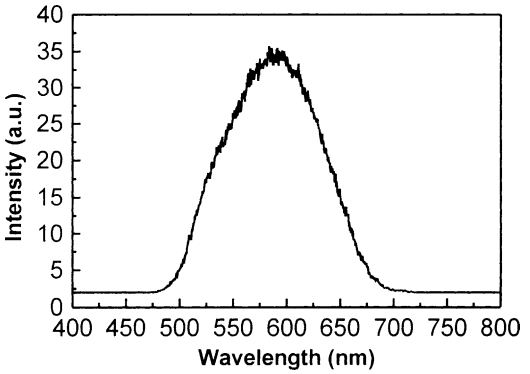

Fig. 3. Upconversion emission spectrum of TiO_2:Mo under 978 nm excitation.

from the t_1 orbital to the 2e orbital, group theory predicts the four excited states $^3T_1, ^3T_2, ^1T_1$ and $^1T_2$, respectively [17]. For TiO_2:Mo sample, the luminescence was assigned to the transitions from the lowest excited states $^3T_1, ^3T_2$ to the ground state $^1A_1$ of the $[MoO_4]^{2-}$ complex.

A phenomenon should be noted that the emission vanishes by heating the materials in oxidizing atmosphere, and then appears again after a subsequent annealing treatment under reducing conditions. The external chemical redox modifying the luminescence means that the Mo^{4+} and Mo^{5+} species caused by the annealing play an important role in the upconversion process. These species may serve as the intermediate states available for upconversion. The excitation mechanism is supposed to be an excited state absorption (ESA) from the intermediate states. This model is enlightened from the one dealing with anti-Stokes emission in undoped YVO_4 [18]. The fluorescence lifetime of the $[MoO_4]^{2-}$ complex was reported in the order of nanosecond [15], we were unable to resolve so fast decay time due to the limitations of our experimental setup. No luminescence was observed from the sample when excited with a pulsed laser (1064 nm) from a Nd:YAG or a pulsed Raman-shift laser (953.6 nm) pumped by a second harmonic of the Nd:YAG. Regardless of the energy mismatch between the pulsed laser and the CW diode laser, the reason may be that the duration time of single laser pulse (10 ns) is much shorter than the rise time of upconversion luminescence where photon avalanche occurs.

3.3. Photon avalanche characterized by power dependence and time evolution

Photon avalanche was first reported in 1979 by Chivian et al. [3]. It is an unconventional continuous wave (CW) pumping mechanism that leads to strong upconverted emission without resonant ground state absorption (GSA). The details about a photon avalanche were described in [8,22].

The 'transfer function' theory for fluorescence dynamics presented by Huang Shi-hua and Lou Li-ren [19] provided an effective method to analyze the kinetics of energy transfer processes in RE-doped crystals [20] and glasses [21]. Here, it is used to characterize the dynamical properties of photon avalanche in TiO_2:Mo. For simplification, we take a three-level system, as presented in Fig. 4. $|0\rangle$, $|1\rangle$ and $|2\rangle$ denote the ground, intermediate and upper excited states, respectively. N_i represents the population of the state $|i\rangle$. We suppose that the transition from $|0\rangle$ to $|1\rangle$ takes place under weak excitation regime, so $N_0 \approx N$, where $N = \sum_{i=0}^{2} N_i \cdot N_2(t)$ describes the population dynamics of the state $|2\rangle$. $\hat{N}_2(s)$ is the direct Laplace transformation of $N_2(t)$. According to the transfer function model, with the excitation of jump function, $\hat{N}_2(s)$ can be written as

$$\hat{N}_2(s) = [F^2\sigma_0\sigma_1 N]/[s[s^2 + (\gamma_2 + \gamma_1 + C + F\sigma_1)s + F\sigma_1(\gamma_{20} - C) + \gamma_1(\gamma_2 + C)]], \quad (1)$$

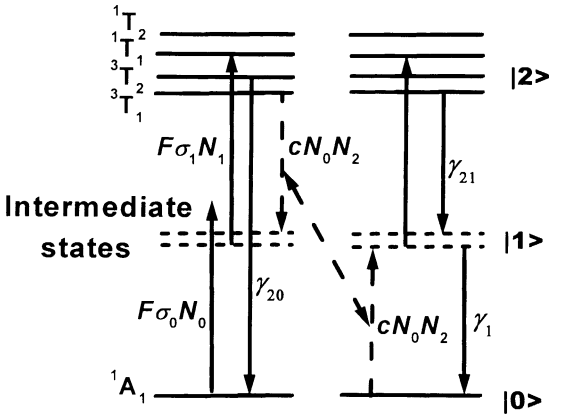

Fig. 4. Energy level and photon avalanche scheme in TiO_2:Mo.

where γ_i is the radiative transition rate of the state $|i\rangle$; γ_{ij} is the transition rate between state $|i\rangle$ and $|j\rangle$; σ_i are the absorption cross-sections; $C = cN$ in which c is the cross-relaxation rate of $(|2\rangle, |0\rangle) \rightarrow (|1\rangle, |1\rangle)$; F denotes the laser-photon density at 978 nm. These quantities are represented schematically in Fig. 4. At steady state, the upconversion-luminescence intensity

$$F_2(\infty) \propto \lim_{t\to\infty} N_2(t).$$

By the rule of Laplace transformation, it can be expressed as

$$F_2(\infty) \propto \lim_{s\to 0} s\hat{N}_2(s) = \frac{F^2\sigma_0\sigma_1 N}{F\sigma_1(\gamma_{20} - C) + \gamma_1(\gamma_2 + C)}. \quad (2)$$

Let

$$\alpha = \frac{\sigma_1(C - \gamma_{20})}{\gamma_1(C + \gamma_2)}, \qquad \beta = \lambda \times \frac{\sigma_0\sigma_1 N}{\gamma_1(C + \gamma_2)},$$

where λ represents the proportionality coefficient. Eq. (2) can be replaced by

$$F_2 = \frac{\beta F^2}{1 - \alpha F}. \quad (3)$$

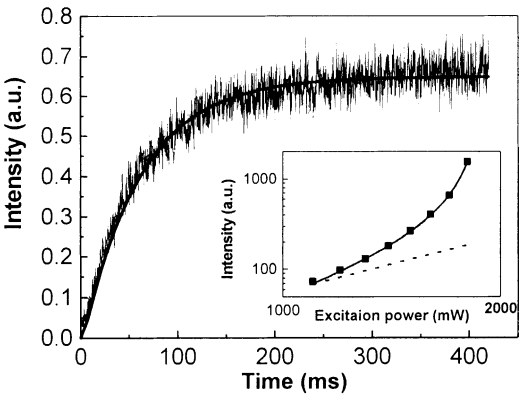

Fig. 5. Time evolution of the upconversion-luminescence intensity of TiO_2:Mo after the onset of 978 nm excitation. The smooth line was calculated by using Eq. (5) and the parameter listed in Table 1. Inset: Double logarithmic plot of upconversion-luminescence intensity vs. excitation power. The solid line was obtained by fitting the experimental data with Eq. (3); the dashed line was calculated by the formula $y = Ax^2$.

Table 1
Parameter values which produced the best agreement between calculated and measured avalanche dynamics

Parameters	α (cm^2 s)	β (cm^2 s)	ρ	χ	τ (ms)
Values	5.3×10^{-4}	2×10^{-5}	0.6515	4.8×10^{-4}	64

The parameters are defined in Eqs. (3) and (5).

In this equation, parameter β was scaled to the measured upconversion-luminescence intensity. β and α were allowed to vary in order to reproduce the experimental data. The inset in Fig. 5 shows the luminescence intensity as a function of the excitation power in a double logarithmic plot. The squares represent experimental data which were well fitted by using Eq. (3), see the solid line in the inset. The parameter values were collected in Table 1. The fitting results suggest $\alpha > 0$, so $C > \gamma_{20}$, i.e., the cross-relaxation process originating from state $|2\rangle$ has a higher probability than radiative or nonradiative relaxation from state $|2\rangle$ to state $|1\rangle$. This satisfies one of the essential conditions needed for the occurrence of photon avalanche [22]. The dashed line in the inset is calculated by the formula $y = Ax^2$, the slope of which is 2. It is obvious that the excitation-power dependence of the upconversion-luminescence intensity in TiO_2:Mo exceeds a quadratic dependence.

To discuss the time evolution behavior of the photon avalanche, we define $\alpha F_{=} 1 - \varepsilon,\ \varepsilon \ll 1$. Eq. (1) is transformed into

$$\hat{N}_2(s) = [F^2\sigma_0\sigma_1 N]/[s[s^2 + (\gamma_2 + \gamma_1 + C + F\sigma_1)s + \varepsilon\gamma_1(\gamma_2 + C)]]. \quad (4)$$

By inverse Laplace transformation, we have

$$N_2(t) \approx \rho[1 + \chi e^{-(t/\chi\tau)} - (1 + \chi)e^{-(t/\tau)}], \quad (5)$$

where

$$\rho = \frac{F^2\sigma_0\sigma_1 N}{\varepsilon\gamma_1(\gamma_2 + C)}, \quad \chi = \frac{\varepsilon\gamma_1(\gamma_2 + C)}{(\gamma_2 + \gamma_1 + C + F\sigma_1)^2},$$
$$\tau = \frac{\gamma_2 + \gamma_1 + C + F\sigma_1}{\varepsilon\gamma_1(\gamma_2 + C)}.$$

Parameter ρ was scaled to the measured luminescence intensity. Fig. 5 shows the rise curve of the upconversion-luminescence intensity of TiO_2:Mo after the switch-on of the 978 nm excitation at $t = 0$. The experimental data is well fitted with Eq. (5), see the smooth line in Fig. 5. The parameter values were listed in Table 1. From the fitting results, χ approaches 0, which means that the second term in Eq. (5), denoting the luminescence-decay component, can be neglected. Parameter τ with a value of 64 ms represents the time constant of luminescence-rise component. The steady-state luminescence is reached after a relatively long time of about 0.3 s. The temporal evolution of the upconversion luminescence, together with the excitation-power dependence of the emission intensity, exhibits the typical fingerprint of a photon avalanche, indicating that the avalanche mechanism predominates in the TiO_2:Mo upconversion. Furthermore, the threshold to start avalanche is roughly determined as 1100 mW from our experiment since the luminescence is too weak to be observed below this value.

4. Conclusions

We developed a new upconversion system TiO_2:Mo presenting visible broadband emission. FTIR spectrum confirms the presence of the $[MoO_4]^{2-}$ complexes, while XPS measurements suggest the co-existence of Mo^{4+} and/or Mo^{5+} species. The luminescence has been assigned to the transitions from the excited states $^3T_1, ^3T_2$ to the ground state $^1A_1$ of the $[MoO_4]^{2-}$ radicle. The Mo^{4+} and/or Mo^{5+} species are supposed to serve as the intermediate states available for upconversion. The temporal evolution of the upconversion luminescence and the excitation-power dependence of the steady-state emission intensity suggest that the photon avalanche occurs in the system. The avalanche dynamics is well described using the fluorescence transfer function model.

Acknowledgements

The authors would like to thank the support of the State Key Project of Fundamental Research of China (G1998061309).

References

[1] T. Sandrock, H. Scheife, E. Heumann, G. Huber, Opt. Lett. 22 (1997) 808.
[2] E. Dowing, L. Hesselink, J. Ralston, R. Macfarlane, Science 273 (1996) 1185.
[3] J.S. Chivian, W.E. Case, D.D. Eden, Appl. Phys. Lett. 35 (1979) 124.
[4] R. Valiente, O.S. Wenger, H.U. Güdel, Phys. Rev. B. 63 (2001) 165102.
[5] U. Oetliker, M.J. Riley, P.S. May, H.U. Güdel, Coord. Chem. Rev. 111 (1991) 125.
[6] D.R. Gamelin, H.U. Güdel, J. Am. Chem. Soc. 120 (1998) 12143.
[7] D.R. Gamelin, H.U. Güdel, Inorg. Chem. 38 (1999) 5154.
[8] M. Wermuth, H.U. Güdel, J. Chem. Phys. 114 (2001) 1393.
[9] D.R. Gamelin, H.U. Güdel, J. Phys. Chem. B 104 (2000) 10222.
[10] A. Conde-Gallardo, M. Garcia-Rocha, I. Hernandez-Calderon, R. Palomino-Merino, Appl. Phys. Lett. 78 (2001) 3436.
[11] Chu-Chi Ting, San-Yuan Chen, Wen-Feng Hsieh, Hsin-Yi Lee, J. Appl. Phys. 90 (2001) 5564.
[12] R.H. Busey, O.L. Kellar, J. Chem. Phys. 41 (1964) 215.
[13] M. Maczka, J. Sol. Stat. Chem. 129 (1997) 287.
[14] W.E. Swartz Jr., D.M. Hercules, Anal. Chem. 43 (1971) 1774.
[15] M. Bohm, A.E. Borisevich, G.Y. Drobychev, A. Hofstaetter, O.V. Kondratiev, M.V. Korzhik, M. Luh, B.K. Meyer, J.P. Peigneux, A. Scharmann, Phys. Stat. Sol. (a) 167 (1998) 243.
[16] R. Kebabcioglu, A. Müller, Chem. Phys. Lett. 8 (1971) 59.
[17] R. Grasser, A. Scharmann, K.-R. Strack, J. Lumin. 27 (1982) 263.
[18] W. Ryba-Romanowski, S. Golab, P. Solarz, G. Dominiak-Dzik, T. Lukasiewicz, Appl. Phys. Lett. 80 (2002) 1183.
[19] H. Shi-hua, L. Li-ren, Acta Phys. Sin. 38 (1989) 422.
[20] A. Brenier, G. Boulon, C. Medej, C. Pedrini, J. Lumin. 54 (1993) 271.
[21] I.R. Martin, V.D. Rodriguez, V. Lavin, U.R. Rodriguez-mendoza, J. Appl. Phys. 86 (1999) 935.
[22] D.B. Gatch, W.M. Dennis, W.M. Yen, Phys. Rev. B 62 (2000) 10790.